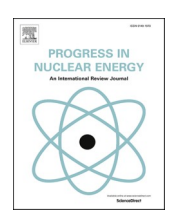
ELSEVIER

Contents lists available at ScienceDirect

Progress in Nuclear Energy

journal homepage: http://www.elsevier.com/locate/pnucene





Optimization of controlling parameters of plasma torch aerosol generator and characteristics of synthesized metal oxide aerosols in context of NAF program

A.K. Dwivedi ^a, Manish Kumar ^b, Gaurav Mishra ^b, Manish Joshi ^c, Arshad Khan ^c, Naveen Tiwari ^d, Sidyant Kumar ^e, T. Saud ^f, B.K. Sapra ^c, S.N. Tripathi ^{a,f,*}

- ^a Department of Civil Engineering, IIT, Kanpur, 208 016, India
- ^b Nuclear Engineering and Technology Programme, Department of Mechanical Engineering, IIT, Kanpur 208016, India
- c Radiological Physics and Advisory Division, Bhabha Atomic Research Centre, Mumbai, 400 085, India
- ^d Department of Chemical Engineering, IIT, Kanpur, 208016, India
- e Department of Aerospace Engineering, IIT, Kanpur, 208 016, India
- f National Aerosol Facility, IIT, Kanpur, 208 016, India

ARTICLE INFO

Keywords: Aerosol characterisation Metal aerosols Morphology Plasma torch aerosol generator Powder feeder TEM YRD

ABSTRACT

The National Aerosol Facility (NAF) has been built at IIT Kanpur, India for studying the aerosol behavior under simulated severe nuclear reactor accident conditions. Plasma torch aerosol generator (PTAG) has been employed in this facility for generating metal oxide particles with desirable properties. Plasma synthesis closely simulates the particle generation characteristics from degraded core during a postulated severe nuclear reactor accident. This study presents the effect of controlling parameters namely electrical power, carrier gas flow rate and powder feed rate of PTAG on the mass characteristics of synthesized metal oxide particles. The structural and morphological information of the synthesized particles has also been obtained via analysis performed using X-ray diffraction (XRD) method and Transmission electron microscopy (TEM). A set of optimized parameters has been finalized based on the outcome of this study. The study aims to standardize the generator system in order to perform future NAF experiments.

1. Introduction

In a severe nuclear reactor accident scenario, fission products in aerosol form are expected to be released from the degraded core of the reactor. The knowledge of the release, transport and retention of these fission products is imperative towards quantifying the amount of radioactivity which could make its way to the environment. Salient features of aerosol dynamics that affects the nature (life and fate) of the aerosols under reactor accident conditions are formation, growth and shape of aerosol particles and their deposition on surfaces (Mishra et al., 2019b). Qualitative as well as quantitative information on the parameters that could influence the aerosol dynamics and on the aerosol characteristics, supplements the probabilistic safety calculations. As the characteristics are expected to be completely different from atmospheric conditions, laws governing the dynamical behavior gets affected as well (Mishra et al., 2019a). The mass concentration in reactor containment

during accident conditions is expected to be around $1 \, g/m^3$ (Sher et al., 1994), much higher than the normal atmospheric conditions. Various experimental facilities/programs have been designed to achieve such characteristics and to address complex mechanisms of particle dynamics and thermal hydraulics simulating conditions as close as possible to the actual reactor accident scenarios (Saraswat et al., 2017). The outcomes of these experimental programs, mainly pertaining to the behavior of aerosols have gained special attention in recent years as they helped in better understanding of the aerosol phenomenon and refining the various available aerosol codes.

Experiments under the DEMONA (DEMOnstration Nuklearen Aerosolverhaltens) (Liljenzin et al., 1990)program were conducted to study the behavior of metal aerosols such as oxides of Sn, Ag, Fe, and Mg, generated using plasma torches in a reasonably large pressurized water reactor (PWR) like containment (640 m^3) and to validate the NAUA code (Bunz et al., 1982). The light water reactor (LWR) aerosol containment

^{*} Corresponding author. Department of Civil Engineering, IIT, Kanpur, 208 016, India. *E-mail address:* snt@iitk.ac.in (S.N. Tripathi).

experiments LACE (LWR Aerosol Containment Experiments) were conducted to investigate aerosol transport and deposition in pipes. Marviken tests (Kljenak and Mavko, 2011) were conducted for investing aerosol transport and deposition along primary cooling components comprising the scrubber, pressurizer relief tank and associated piping system. The ultimate goal of these experiments and phenomenology describing the behavior of aerosol released in a reactor accident is to develop calculation tools that can predict the characteristics of the aerosol particles which may get released to the external environment in unlikely scenario of an accident. Aerosol generator is one of the key components of these experimental facilities. To generate airborne particles and to transport the same to various experimental facilities, a multi purpose aerosol generation facility DRAGON (DiveRse purpose Aerosol GeneratiON facility) (Suckow and Guentay, 2008) was established. It is being used for the generation of particles of different sizes and characteristics utilizing plasma torches, fluidized bed generators, two-fluid nozzles, atomizers and dry powder feeders. It has been widely used in facilities such as CONGA (Containment behaviour in the event of core melt with large gaseous and aerosol releases), POSEIDON (Pool Scrubbing Effect on Iodine Decontamination), ARTIST (Aerosol Trapping In a Steam Generator) and VEFITA (Venting Filter Assessment) for different purposes in varied research contexts. A medium-scale facility named as Nuclear Aerosol Test Facility (NATF) was built at Bhabha Atomic Research Centre for carrying out aerosol behavior experiments under simulated reactor accident conditions. The experiments carried out in this facility focused on the evolution of spatial distribution of aerosol mass concentration and size distribution, measurement of particle densities, and study of deposition and depletion characteristics in the test vessel and piping assemblies (Sapra et al., 2008; Modi et al., 2014; Dwivedi et al., 2019).

National Aerosol Facility (NAF), a multipurpose facility has been built at Indian Institute of Technology, Kanpur, India. Experiments to be conducted in this facility aim to study spatial and temporal evolution of metallic particles in different test components (large sections of pipes and scale down containment) incorporating deposition and resuspension dynamics. These experiments are to be performed in dry and wet conditions, mainly to simulate severe nuclear accident scenario for Indian PHWR (Pressurized Heavy Water Reactor). Loss of coolant accident (LOCA) in primary heat transport (PHT) system has been taken into consideration while simulating severe accident for the present context. At present, this facility comprises of advance aerosol generation system, steam generation and non condensable feed system, mixing chamber and piping assemblies (varying cross-section, parallel paths, bends, elbows, etc). Advanced instrumentation e.g. Scanning mobility particle sizer (SMPS), Hygroscopic Tandem Differential Mobility Analyser (HTDMA), Phase Doppler Particle Analyzer (PDPA), Cloud Condensation Nuclei Counter (CCNC), Impactors and high temperature sampling devices are intended to be used for measurement and characterization of the aerosol properties/behaviour during experiments planned in this facility. Additionally, various conventional process instrumentation are planned to be used for monitoring the process variables i.e. pressure, temperature, gas flow, steam flow, steam concentration etc. This medium scale facility aims to create extensive experimental database against test matrix designed to cover diverse parametric changes of aerosol particles in dry and wet conditions. This helps in validating and strengthening the prediction capabilities of the aerosol simulation codes in context of safety assessment of Indian PHWR reactors. Usage of state of the art aerosol instrumentation and relatively large test sections (pipes and chamber) makes it one of a kind for studying medium or large scale aerosol effects which otherwise are not studied in depth in laboratory conditions. The facility is equipped to perform complex and diverse aerosol experiments namely deposition in complex structures, re-suspension phenomenon, mixed aerosol behavior in condensing environment and effect of charge on the interaction mechanisms etc.

Out of different techniques of aerosol generation (evaporationcondensation, fluidized bed and atomization based methods), evaporation-condensation technique is most commonly used for generating metal aerosols in large scale facilities (Hutcheon et al., 2003; Suckow and Guentay, 2008). The high concentration from this kind of generator system best simulates the aerosol generation during the core degradation that can occur in a postulated severe nuclear reactor accident. In this technique, the metal powder is first evaporated at very high temperature and the hot vapors are then transported to the colder regions by a carrier gas. These vapors begin to nucleate in such conditions generating primary particles which finally evolve to higher sizes depending on the residence time. It is found that cooling of the vapor is very fast and due to high supersaturation, homogeneous nucleation is a predominant path for vapor condensation rather than heterogeneous nucleation (Girshick, 1994). PTAG not only yields an intense and continuous aerosol stream but can also generate aerosols from a wide variety of materials such as metals, ceramics, and composites. Plasma synthesis is carried out using a Plasma Torch (PT) which produces a steady thermal plasma jet by passing a high current through a working gas, typically an inert gas such as argon or helium. In recent decades, non-transferred DC plasma torches have been used as an effective heat source for the production of metal powders. Since the temperatures in a thermal plasma are very high (> 10⁴ K), chemical reactions are much more energetic than those encountered in conventional processes (Sreekumar et al., 1996).

This work focuses on the optimization of working parameters of PTAG for controlling the mass characteristics of synthesized metal oxide (ZnO and SnO) particles. The plasma torch was operated at different powers and carrier gas flow rates and mass characteristics (mass concentration and mass size distribution) were measured and interpreted. The powder feeder was also calibrated in terms of mass flow rate (powder obtained) for different metal aerosols. The plasma synthesized particles were also characterized using X-ray diffraction and TEM analysis for their morphology. The optimized parameters and the consequent aerosol characteristics will be serving as a crucial database for the future NAF experiments.

2. Materials and methods

2.1. Experimental setup

The experiments were performed in NAF facility which is a largescale facility for carrying out aerosol behaviour experiments under simulated severe nuclear accident conditions. The experimental set-up consists of a Plasma Torch Aerosol Generator, a powder feeder, carrier gas delivery system, sealed plexiglass chamber, chiller unit and aerosol sampling devices. The chamber is made up of plexiglass having volume of 1.25 m^3 (length 1.0 m, width 1.0 m and height 1.25 m) with multiple ports on walls and base for inserting the thermocouples. A fan (diameter 12 inches) operating at 900 RPM (revolutions-per-minute) is installed at the center of the ceiling to avoid the localized heating and for ensuring homogeniety of sample in the chamber. Powder feeder (model: MEC PF-3350), was used for injecting the metal powder on the plasma flame at a constant feed rate. Stainless steel pipe of length 1 m was used to transport the generated metal aerosols to plexiglass chamber. It also acted as pipe section of test setup with multiple ports for inserting the thermocouples and for extracting the aerosol samples. The pipe section was cooled by winding copper tubes to prevent it from excessive heating. A cooled water from the chiller unit was circulated inside the copper tubes to restrict damage of pipe section near plasma flame. Factory-calibrated K-type thermocouples were used for measurement of temperature, and the data was recorded through data logger (model:YCT-747UD). A 47 mm filter holder, made of stainless steel, was used to measure the gross mass concentration (without size separation) (Khandare et al., 2016; Joshi et al., 2011) and Micro-Orifice Uniform Deposit Impactor (MOUDI, model:100 NR) was used to collect size-fractionated aerosol particles for gravimetric analyses. MOUDI works on the principal of inertial impaction and separates particles according to their aerodynamic diameter

range which has 8 stages in which upper three stages were operating at normal pressure and lower four stages were at low pressure (150 mm Hg). Aerodynamic size cuts for this impactor are 0.18, 0.32, 0.56, 1.0, 1.8, 3.2, 5.6, 10 and 18 μ m with sampling flow rate of 30 $Lmin^{-1}$. The detailed schematic diagram of the experiment setup is shown in Fig. 1.

2.1.1. Plasma torch aerosol generator (PTAG)

The plasma torch aerosol generator used in this study is of nontransferred type. It has a rod type cathode, made of tungsten of 6 mm diameter with its end made of thoria for better thermionic emission while the anode is made of copper, in the form of convergent nozzle with a conical shape. To avoid overheating of nozzle due to arc bending, centering of the cathode with respect to the anode is crucial and it was well aligned in the present case. The entire PTAG assembly (cathode and anode) is cooled by chilled water circulated from separate chiller unit through circulation pumps. Similar type of PTAG was used for generating metal aerosols for piping and containment experiments at NATF (Sapra et al., 2008). The arc generated from the PTAG (shown in Fig. 2) strongly depends on the nozzle design like its diameter and operating parameters viz. arc current, voltage and mass flow rates of gas. Structure of an arc is also dependent on the gas used for plasma generation as different gases have different specific heats, thermal conductivities, radical production and power requirements (Ohno, 1984). In present study, argon gas is used as primary plasma gas for plasma generation and once the flame is stabilized, nitrogen gas is added to increase its enthalpy.

2.1.2. Powder feeder

The powder feeder (model: MEC PF-3350) was used for feeding metal powders on plasma flame in the present work, which works on pressurization and constant volumetric feed principle. The powder is stored in a pressurized canister which can withstand a backpressure of 7.5 bar and a slotted metal disc is mounted off-center at the bottom of it.



Fig. 2. A typical plasma arc photographed at the power 25 kW.

A fixed amount of powder fills inside each slot, and as the disc rotates, this powder is fed into the powder hose and then to the spray gun. A moter drive having digital RPM display governs the speed of rotating disk which is proportional to the powder obtained. This powder feeder can be used manually as well as automatically with the Programmable Logic Controller (PLC) system.

2.2. Experimental procedure

Experiments were performed at three different powers of PTAG (15, 25, 35 kW) and at each power three carrier gas flow rates (100, 150, 200 $Lmin^{-1}$) were selected to investigate the effect of PTAG power and carrier gas flow rates on size of the generated metal aerosols. The flow rates 100, 150 and 200 $Lmin^{-1}$ corresponds to residence times of 5, 4.2 and 3 s

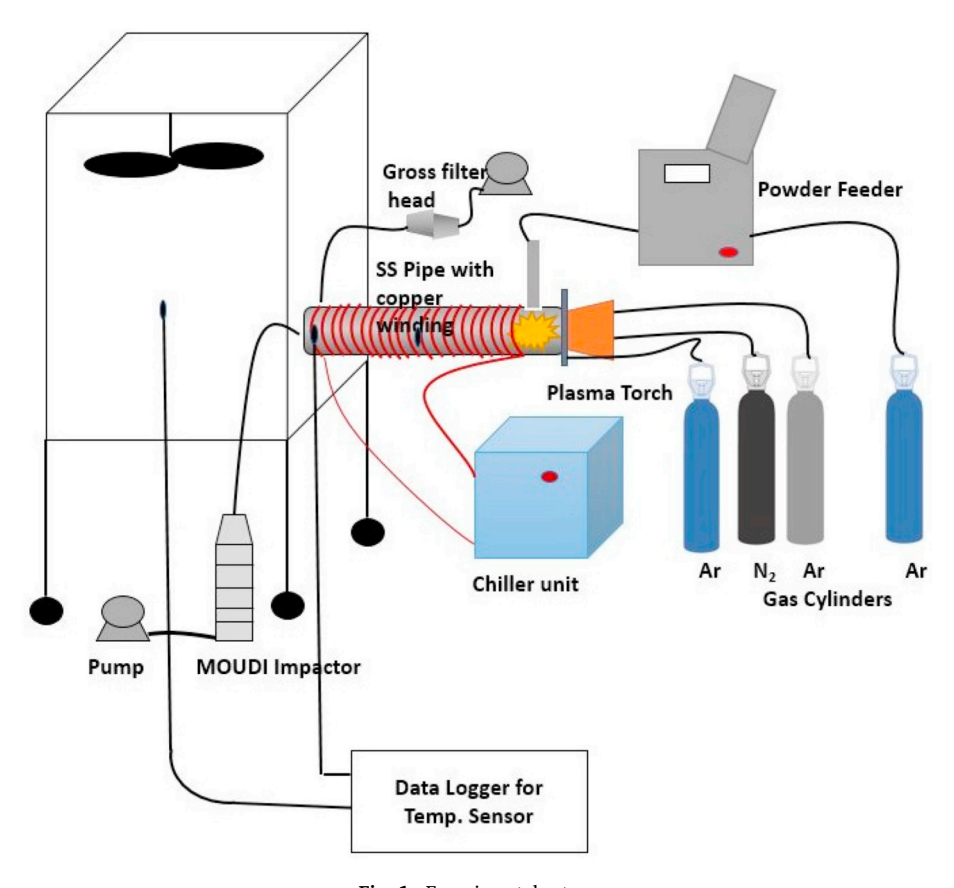


Fig. 1. Experimental setup.

respectively inside the pipe section. The flow conditions in these test experiments were maintained in laminar region so as not to disturb the characteristics of the exit particles from PTAG. However, once these particles are fed to the test section, flow conditions could be turbulent as well. Several pilot experiments were carried out in order to standardize the aerosol generation parameters like powder feed rate, plasma torch operating power, flow rates of plasma gases etc. The pilot experiments helps us in selecting a suitable duration and sampling flow rates for the experiment such that there would be no choking of aerosol instrumentation viz. MOUDI impactor, gross filters etc., and at the same time ensuring sufficient deposition on the filter papers for correct estimation of the mass concentration. It was found out that at low PTAG power below 10 kW the metal powder couldn't be aerosolized properly resulting in highly unburnt metal powder at the pipe outlet. At high PTAG power (above 35 kW) the high temperature leads to melting of copper cathode of PTAG and contaminating the test aerosols with it. The low carrier gas flow rate (below 100 Lmin⁻¹) results in the more residence time of aerosols in pipe section leading to increased particle sizes due to coagulation. A minimum carrier gas flow rate of around 100 *Lmin*⁻¹ provides sufficient momentum to the generated aerosol so that it can be easily transported to large distance in piping sections. Details of parameters used in all experiments are provided in Table 1. To achieve high PTAG power, nitrogen gas flow rate to the PTAG was raised to 10 $Lmin^{-1}$.

At the beginning of each experiment, the entire chamber and pipe section were cleaned with a wet cloth to minimize the total background aerosol concentration. After that all the openings in the chamber were kept closed to minimize the transport of ambient aerosol particles inside the chamber. With the use of HEPA filters, clean air was blown into the chamber using centrifugal pumps to evacuate the chamber and to minimize the ambient particle concentration inside the chamber. Condensation Particle Counter (CPC, TSI 3776) and Aerodynamic Particle Sizer (APS, TSI 3321) were used to ensure the zero particle concentration inside the entire test setup. Argon gas was used to act as powder feeder gas to transport the metal powder kept in the powder feeder into the plasma flame. Generated metal oxide aerosols were transported into the plexiglass chamber assembly using nitrogen as carrier gas. After firing the plasma torch, first 60 sec were given to stabilize plasma flame and once the flame gets stabilized the powder feeder was turned on.

The measurements were started after 2 min from beginning just to ensure sufficient aerosol mass concentration via visual inspection. Aerosol sampling was carried out from the outlet of the pipe section using the gross filter paper sampler and MOUDI impactor for the estimation of the total mass concentration and mass size distribution respectively. The total sampling time for the measurements was 1 min for both gross filter paper sampler and MOUDI impactor. The mass size distribution of the aerosol collected by the MOUDI stages was determined by weighing the filters using a high-precision micro balance

Parameters used for experiment.

Parameters	Exp-(15 kW)	Exp-(25 kW)	Exp-(35 kW)
Powder used Total flow rate of carrier gas $(Lmin^{-1})$	Zinc,Tin 100, 150, 200	Zinc,Tin 100, 150, 200	Zinc,Tin 100, 150, 200
Run Time (min)	6.0	6.0	6.0
Argon flow rate for torch $(Lmin^{-1})$	25.0	25.0	25.0
Nitrogen flow rate for torch ($Lmin^{-1}$)	5.0	5.0	10
Argon flow rate for powder feeder $(Lmin^{-1})$	10.0	10.0	10.0
Powder feed rate (gmin ⁻¹)	1.0	1.0	1.0
Total weight of powder aerosolized (g)	6.0	6.0	6.0

(model: M3P-000V001, Sartorius). Prior to weighing, the filters were equilibrated for 24 h inside the desiccator. At the end of each set of experiment, the plasma torch was turned off, the test section was left for cooling. The collected samples from MOUDI impactors were analyzed gravimetrically for mass size distribution. The samples deposited on gross filters were analyzed using Transmission Electron Microscopy (TEM) and X-ray Diffraction (XRD) techniques.

3. Results and discussion

As discussed earlier, PTAG experiments were performed in order to optimize the operational parameters and to characterize the generated aerosol particles. The essential parameters under investigation are operative electrical power, carrier gas flow rate and powder feed rate (to the plasma zone). The examined PTAG powers were 15, 25, 35 kW and carrier gas flow rates were 100, 150, 200 *Lmin*⁻¹, respectively. Thermodynamic conditions during entire set of experiments are presented in Table 2. These include the temperature of the carrier gas measured at the outlet of the piping section (see Fig. 1). Maximum temperature of 1063 K was recorded for the case of 35 kW PTAG power at 100 Lmin-1 carrier gas flow rate. It is also apparent that the calculated flow Reynold's number during these experiments were in laminar region only.

3.1. Powder feeder calibration

The powder feeder was calibrated using two different metal powders, Zinc and Tin, for fixed gas flow rate of 10 Lmin⁻¹. The mesh size of examined metal powders was 325 which corresponds approximately to size of 45 µm. Fig. 3 represents the relationship between powder obtained and revolution per minute (RPM) of rotating disk (of feeder) for metal powders (Zinc and Tin). For tin metal, powder obtained was seen to be varying linearly within experimental uncertainty in the tested RPM ranges. For zinc metal, obtained powder rate was seen to be saturating for higher RPMs and was best fitted with a parabolic equation. It was also observed that varying the gas flow rate from 10 to 30 Lmin-1 of powder feeder has no effect on the mass flow rate from the feeder. Three sets of experiments were performed at each RPM and a good repeatability was observed. Although powder feeder could be used for any tested RPM, PTAG characterization experiments in this work were performed with 0.15-0.20 RPM. This was done to ensure that the powder obtained from the feeder or powder input to plasma torch is approximately 1.0 (*gmin*⁻¹). This level corresponds to the mass concentrations which are typical representative for reactor accident scenario simulations. However, aerosol generation rate can be increased by increasing RPM for experiments where higher mass concentration is desired.

3.2. Temperature profiles

The temperatures were measured at the pipe outlet near the sampling port and at different locations inside the plexiglass chamber. Fig. 4

Table 2Thermo-dynamic conditions during experiment.

			-		
Experiment (PTAG power)	Carrier gas	Flow rate (<i>Lmin</i> ⁻¹)	Maximum temperature of carrier gas at outlet (K)	Average velocity at outlet (ms ⁻¹)	Flow Reyonld's number (<i>Re</i>)
Exp-(15 kW)	Nitrogen	100	688	0.175	432
		150	643	0.237	585
		200	593	0.300	740
Exp-(25 kW)	Nitrogen	100	930	0.175	212
		150	913	0.237	288
		200	905	0.300	365
Exp-(35 kW)	Nitrogen	100	1063	0.175	180
- '	· ·	150	1033	0.237	244
		200	1013	0.300	308

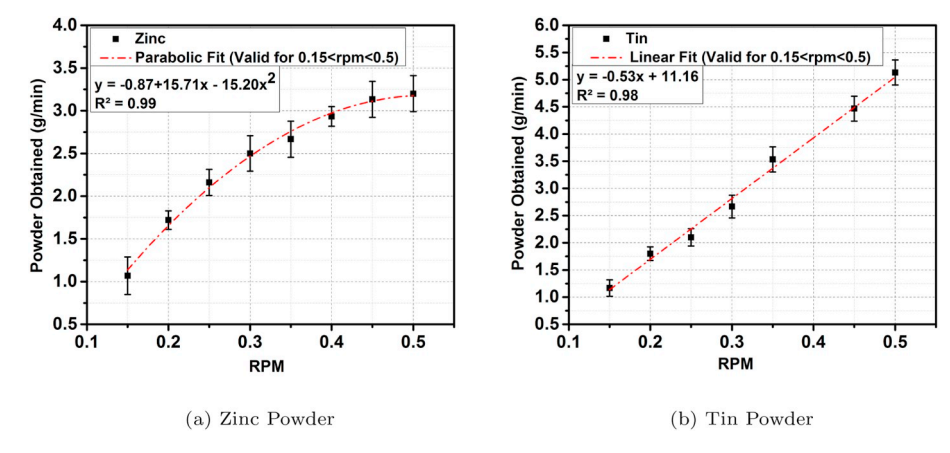


Fig. 3. Powder obtained vs RPM (a) Zinc metal powder (b) Tin metal powder.

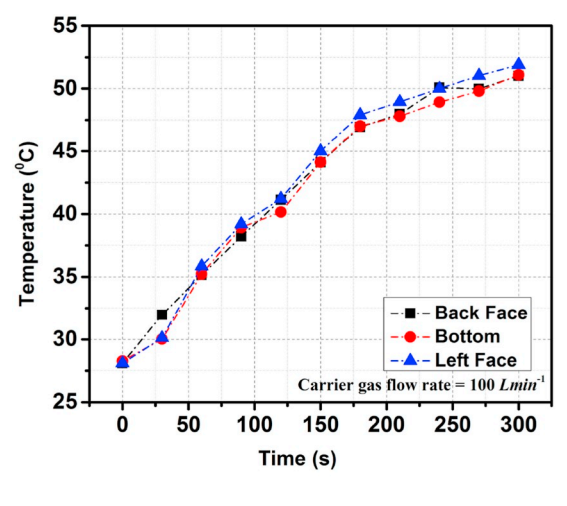
(a) shows temperature profiles at bottom and side faces of plexiglass chamber. The temperature increases with time and reaches to a maximum of 50 °C by the end of each test run for a carrier gas flow rate of 100 *Lmin*⁻¹ and PTAG power of 25 kW. To ensure the safe operational limit of aerosol instrumentation and plexiglass chamber, temperature profiles for various PTAG powers (15, 25, 35 kW) were measured and the results were presented in Fig. 4 (b) for 100 Lmin⁻¹ carrier gas flow rate. With the increase in PTAG power, the temperature increases at pipe outlet location and reaches to a maximum of 800 °C (for 35 kW case). The saturation temperature value measured for 35 kW PTAG power was observed to be almost double of that measured for 15 kW PTAG power for other similar conditions. It was observed that temperature rises sharply from room temperature and attains almost constant value after 100 s of operation for all experiments as shown in Fig. 4 (b). The temperature inside the plexiglass chamber was very low as compared to the pipe outlet because of both uniform mixing inside and loss of heat from the chamber.

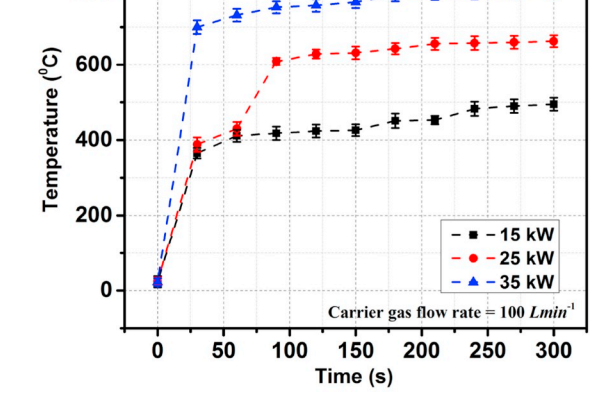
3.3. Size distribution measurements

Mass Median Aerodynamic Diameters (MMADs) were calculated for both Zinc and Tin metal powders at outlet of pipe under different carrier gas flow rates as well as for different PTAG power conditions. These estimations were made from the mass size distribution function measured by MOUDI impactor for all these cases. The MMAD plots of Zinc and Tin metal for a single set of experiment has been shown in Fig. 5. Table 3 shows the average MMAD and GSD obtained graphically for different carrier gas flow rates and PTAG powers. Each set of experiment was repeated three times to check reproducibility of results and averages of these three sets are presented. For a fixed PTAG power, MMAD decreases with the increase in carrier gas flow rate, which can be attributed to less residence time for agglomeration of the particles as they travel along the pipe length. This behaviour was seen at all examined PTAG powers for both Zinc and Tin aerosols.

With increase in PTAG power there was slight increment in MMAD for all observed carrier flow rates. Increase in PTAG power leads to complete vaporization of metal powder, which results in high particle number concentration of generated aerosols. It is well known that coagulation effect is more dominating at higher particle number concentration (Anand et al., 2012; Sapra et al., 2008) which is responsible for larger MMAD at higher PTAG power. Average MMAD lies between 0.22 μm to 0.35 μm which is in good agreement with the size generated from PTAG, measured in POSEIDON facility (Dehbi et al., 2001; Suckow and Guentay, 2008).

Table 4 shows the total mass concentration of zinc and tin particles measured using gross filter and average mass concentration of $0.81\ g/m^3$ was obtained in various sets of performed experiments. The average mass concentration for zinc aerosol was observed to be higher then that of tin aerosol. This could be because of the larger size (MMAD) of generated zinc particles. Similar total mass concentration value is also





(a) Inside the plexiglass chamber

(b) At pipe outlet

Fig. 4. Temperature profile (a) At different locations inside the plexiglass chamber for gas flow rate of $100 \, Lmin^{-1}$ and PTAG power of $25 \, kW$ (b) At pipe outlet for gas flow rate of $100 \, Lmin^{-1}$

800

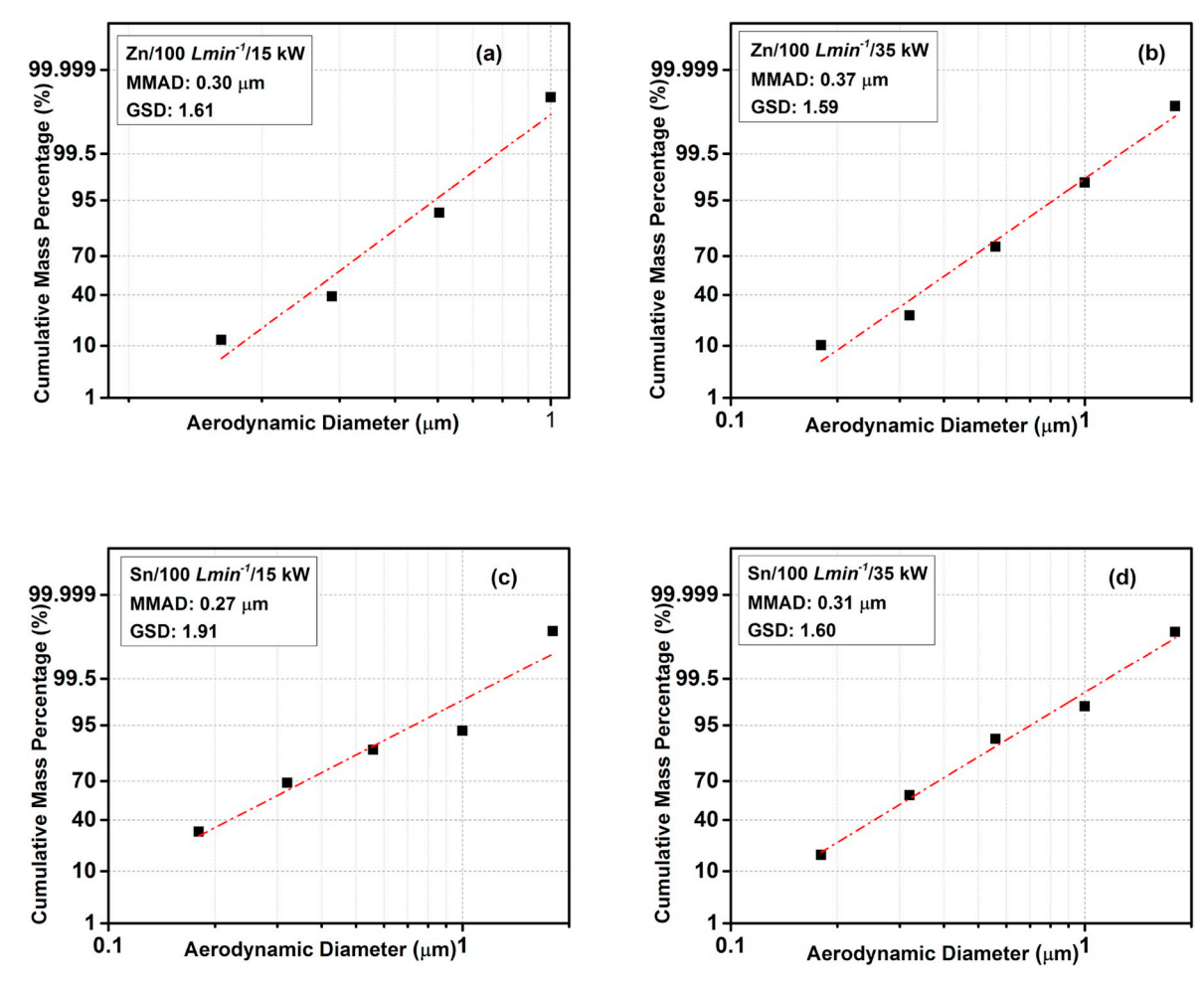


Fig. 5. Aerosol mass size distribution for Zinc (a, b) and Tin (c, d) for PTAG power 15 kW, 35 kW and carrier gas flow rate 100 Lmin⁻¹

Table 3Average MMAD and GSD for different carrier gas flow rates and PTAG power.

Flow (Lmin ⁻¹)	15 (kW)	25 (kW)	35 (kW)
	MMAD (μm) GSD	MMAD(μm) GSD	MMAD (μm) GSD
Zinc (Zn)			
100	$0.29 \pm 0.071.61 \pm 0.00$	$0.34 \pm 0.061.69 \pm 0.03$	$0.35 \pm 0.031.63 \pm 0.04$
150	$0.29 \pm 0.041.71 \pm 0.06$	$0.33 \pm 0.071.55 \pm 0.07$	$0.34 \pm 0.031.69 \pm 0.11$
200	$0.23 \pm 0.041.92 \pm 0.12$	$0.26 \pm 0.001.76 \pm 0.00$	$0.26 \pm 0.031.86 \pm 0.06$
Tin (Sn)			
100	$0.27 \pm 0.041.64 \pm 0.27$	$0.33 \pm 0.021.73 \pm 0.12$	$0.34 \pm 0.061.64 \pm 0.09$
150	$0.25 \pm 0.001.80 \pm 0.10$	$0.29 \pm 0.051.70 \pm 0.17$	$0.30 \pm 0.031.75 \pm 0.95$
200	$0.22 \pm 0.031.60 \pm 0.10$	$0.24 \pm 0.021.75 \pm 0.13$	$0.25 \pm 0.021.67 \pm 0.15$

Table 4 Total mass concentration (g/m^3) obtained in various sets of experiment.

Flow ($Lmin^{-1}$)	15 (kW)	25 (kW)	35 (kW)	
	Mass Conc. (g/m^3)	Mass Conc. (g/m^3)	Mass Conc. (g/m^3)	
Zinc (Zn)				
100	0.894 ± 0.231	1.001 ± 0.275	$\boldsymbol{0.908 \pm 0.364}$	
150	$\boldsymbol{1.129 \pm 0.197}$	$\boldsymbol{1.200 \pm 0.206}$	$\boldsymbol{1.098 \pm 0.382}$	
200	$\boldsymbol{0.768 \pm 0.114}$	$\boldsymbol{0.638 \pm 0.213}$	$\boldsymbol{0.728 \pm 0.152}$	
Tin (Sn)				
100	$\boldsymbol{0.749 \pm 0.282}$	0.777 ± 0.180	0.527 ± 0.039	
150	$\boldsymbol{0.637 \pm 0.094}$	$\boldsymbol{0.728 \pm 0.034}$	0.773 ± 0.172	
200	$\boldsymbol{0.473 \pm 0.100}$	0.611 ± 0.122	0.889 ± 0.273	

observed in study performed by (Dwivedi et al., 2019) for a feeding rate of 1.0 ($gmin^{-1}$)

3.4. XRD and TEM analysis

The collected metal oxide particles on the filters were characterized using X-ray diffraction (XRD) technique for determining the crystalline phases and their approximate proportions by examining the respective diffraction patterns. A copper-Ka source (40 kV; 40 mA) and a Lynx Eye 1D detector with a discrimination voltage range of 0.18 - 0.25V were used in the current study. Phase identification is usually made by employing the ICDD (International Center for Diffraction Data) diffraction database, which catalogs the X-ray diffraction patterns of

thousands of crystals. Fig. 6,(a) and (b) show X-ray diffraction pattern of sampled metal aerosol particles. The diffraction peaks can be indexed to ZnO and SnO showing their formations. No peaks corresponding to Zn and Sn were observed, which confirms that no unburnt metal particles were present.

The Transmission Electron Microscopy (TEM) analysis were done to obtain shape and size of aerosolized metal particles. TEM was carried out using FEI Tecnai G^2 F20 transmission electron microscope available in the Advanced Imaging Centre at IIT Kanpur. The samples for TEM measurements were prepared from very diluted dispersions of the particles in 2-propanol the conventional 200 mesh size carbon coated copper grids were used as a support. Fig. 7 (a), (b) shows the TEM images of deposited Zinc oxide particles and Fig. 7(c) and (d) shows the same for Tin oxide particles.

When examined under via TEM, both metal oxide particles were seen to consist of agglomerates of primary particles of diameter < 100 nm. ZnO particles were observed rod-shaped, flake-like and crystalline while SnO particles were nearly spherical and quite monodisperse. The agglomerates appear fairly solid in nature, with no sign of the hollow spheres. Mostly the size of particles for both metal oxides were observed between 5 and 50 nm. Similar size range of the metal oxide particles were obtained by (Modi et al., 2014) for the plasma generated metal aerosol. It is also accepted that the formation of metal aerosol through rapid cooling favors homogeneous over heterogeneous condensation, resulting in particle with sizes in the 10 nm range (Oxtoby and Evans, 1988). Observed shape can be used for modelling the early growth of the particles by predicting the shape factor. The shape factors also influence thermophoretic and gravitational deposition rates, as well as agglomeration rates. It is also possible (and planned) to model drag force utilizing the positions if all primary particles observed in a typical nanocluster.

4. Summary and conclusion

In the present study, characterization of PTAG at NAF, IIT Kanpur has been done. Various parameters such as PTAG power, carrier gas flow rate, powder feed rate through powder feeder have been examined to obtain suitable operational optimized parameters for the future experiments. The powder feeder has been calibrated using zinc and tin metal powders and results shows that for tin metal, obtained powder varies linearly within experimental uncertainty in the tested RPM ranges. For zinc metal, obtained powder rate was seen to be saturating for higher RPMs and was best fitted with a parabolic equation. The desired powder mass flow rate from powder feeder was obtained at rotating disk's RPM of 0.15-0.2. Mass characteristics of aerosols were measured for both powders in terms of integral mass concentration and mass size distribution. The MMAD has been estimated for different carrier gas flow rates and PTAG powers. At higher carrier gas flow rate, the average MMAD was observed to be smaller as compared to lower carrier gas flow rate. The same behavior has been observed for all examined PTAG powers. The average MMAD size range of the generated metal aerosol has been found to be 0.22 µm to 0.35 µm. X-ray diffraction (XRD) of collected samples showed the formation of oxides of zinc and tin, which is expected for the plasma torch generated aerosols under atmospheric conditions as discussed in previous studies (Modi et al., 2014; Dwivedi et al., 2019). TEM analysis of the generated metal aerosol reveals that the shape of tin aerosol are mostly spherical while that of Zinc is cylindrical, rod-shaped and flake-like. The size range of the spherical aerosol particles was noted between 5 nm and 50 nm. The observed shape can be used for modelling the early growth of the particles by predicting the shape factor. The interpretations made from the results obtained during the experiments conducted under this work could be instrumental for future NAF experiments. Desired aerosol characteristics can be achieved by tuning operational parameters of PTAG as per the test matrix and the context.

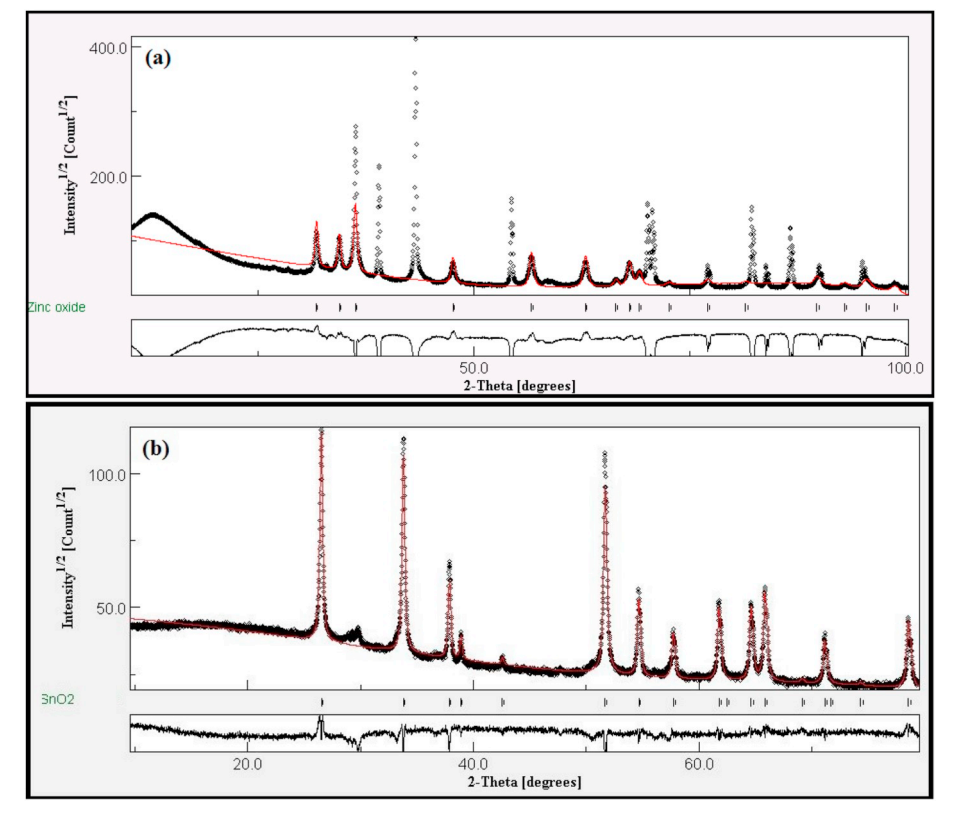


Fig. 6. XRD pattern for (a) Zinc oxide particles (b) Tin oxide particles.

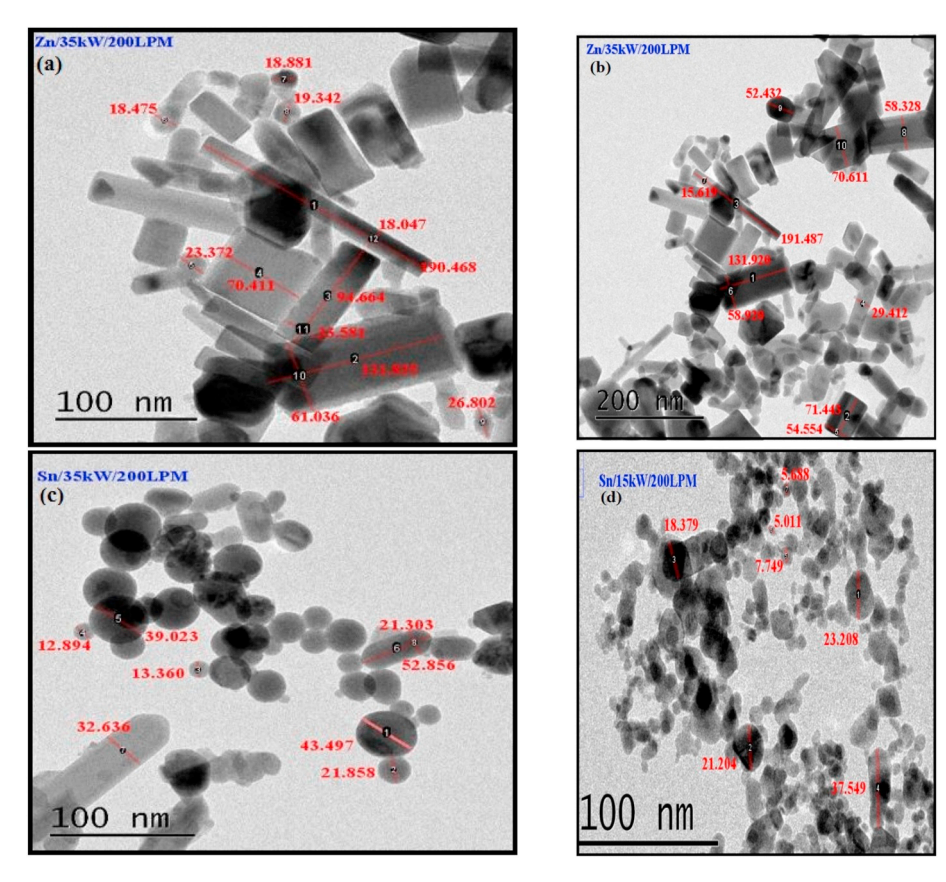


Fig. 7. TEM micrographs for Zinc particle (a, b) and Tin particle (c, d).

CRediT authorship contribution statement

A.K. Dwivedi: Conceptualization, Methodology, Validation, Investigation, Writing - original draft. Manish Kumar: Validation, Investigation, Visualization. Gaurav Mishra: Methodology, Validation, Investigation, Writing - review & editing. Manish Joshi: Methodology, Data curation, Writing - review & editing, Supervision. Arshad Khan: Conceptualization, Data curation, Writing - review & editing, Supervision. Naveen Tiwari: Writing - review & editing, Supervision. Sidyant Kumar: Validation, Investigation. T. Saud: Investigation, Writing - review & editing. B.K. Sapra: Resources, Supervision, Funding acquisition, Project administration. S.N. Tripathi: Conceptualization, Resources, Supervision, Project administration, Funding acquisition.

Acknowledgment

The authors also gratefully acknowledge the financial support provided by Board of Research in Nuclear Science (BRNS), Department of Atomic Energy (DAE), Government of India to conduct this research under project no. 36(2,4)/15/01/2015-BRNS.

Appendix A. Supplementary data

Supplementary data to this article can be found online at https://doi.org/10.1016/j.pnucene.2020.103311.

References

Anand, S., Mayya, Y., Yu, M., Seipenbusch, M., Kasper, G., 2012. A numerical study of coagulation of nanoparticle aerosols injected continuously into a large, well stirred chamber. J. Aerosol Sci. 52, 18–32.

Bunz, H., Koyro, M., Schoeck, W., Mod, N., 1982. 4: a code for calculating aerosol behaviour in lwr core melt accidents. In: Code Description and Users' Manual," Unpublished Preliminary Description Presented at a Workshop Held at EPRI. California, Palo Alto.

Dehbi, A., Suckow, D., Guentay, S., 2001. Aerosol retention in low-subcooling pools under realistic accident conditions. Nucl. Eng. Des. 203 (2–3), 229–241.
Dwivedi, A.K., Khan, A., Tripathi, S., Joshi, M., Mishra, G., Nath, D., Tiwari, N., Sapra, B., 2019. Aerosol depositional characteristics in piping assembly under varying flow conditions. Prog. Nucl. Energy 116, 148–157.

Girshick, S.L., 1994. Particle nucleation and growth in thermal plasmas. Plasma Sources Sci. Technol. 3 (3), 388.

Hutcheon, D., Bishop, S., Buchmann, L., Chatterjee, M., Chen, A., D'Auria, J., Engel, S.,
 Gigliotti, D., Greife, U., Hunter, D., et al., 2003. The dragon facility for nuclear astrophysics at triumf-isac: design, construction and operation. Nucl. Instrum.
 Methods Phys. Res. Sect. A Accel. Spectrom. Detect. Assoc. Equip. 498 (1–3),

Joshi, M., Sapra, B., Kothalkar, P., Khan, A., Modi, R., Mayya, Y., 2011. Implications of polarity of unipolar ionisers on reduction of effective dose attributable to thoron progeny. Radiat. Protect. Dosim. 145 (2–3), 256–259.

Khandare, P., Joshi, M., Khan, A., Sapra, B., Mayya, Y., 2016. Ionizer induced 220rn decay product removal in confined environment: continuous vs. instantaneous source. J. Environ. Radioact. 164, 182–189.

Kljenak, I., Mavko, B., 2011. Simulation of containment thermal-hydraulics in the marviken blowdown 16 experiment with astec and contain codes. Nucl. Eng. Des. 241 (4), 1063–1070.

Liljenzin, J., Collen, J., Schock, W., Rahn, F., 1990. Report from the marviken-v: Demona: lace workshop. In: Proceedings of the Workshop on Aerosol Behaviour and Thermal–Hydraulics in the Containment. CSNI Report number 176.

Mishra, G., Mandariya, A.K., Tripathi, S., Joshi, M., Khan, A., Sapra, B., et al., 2019a. Hygroscopic growth of csi and csoh particles in context of nuclear reactor accident research. J. Aerosol Sci. 132, 60–69.

Mishra, G., Tripathi, S., Saud, T., Joshi, M., Khan, A., Sapra, B., 2019b. Study on Ccn Activity of Fission Product Aerosols (Csi and Csoh) and Their Effect on Size and Other Properties. Atmospheric Research, p. 104816.

Modi, R., Khan, A., Joshi, M., Ganju, S., Singh, A.K., Srivastava, A., Sapra, B.K., Mayya, Y. S., 2014. Metal oxide aerosol dry deposition in laminar pipe flow at high thermal gradients and comparison with sophaeros module of astec reactor accident analysis code. Ann. Nucl. Energy 64, 107–113.

Ohno, S., 1984. Generation rate of ultrafine metal particles in" hydrogen plasma-metal" reaction. J. Jpn. Inst. Metals 48, 640–646.

Oxtoby, D.W., Evans, R., 1988. Nonclassical nucleation theory for the gas-liquid transition. J. Chem. Phys. 89 (12), 7521–7530.

Sapra, B.K., Mayya, Y.S., Khan, A., Sunny, F., Ganju, S., Kushwaha, H.S., 2008. Aerosol studies in a nuclear aerosol test facility under different turbulence conditions. Nucl. Technol. 163 (2), 228–244.

- Saraswat, S., Munshi, P., Khanna, A., Allison, C., 2017. Thermal hydraulic and safety assessment of first wall helium cooling system of a generalized test blanket system in iter using relap/scdapsim/mod4. 0 code. J. Nucl. Eng. Radiat. Sci. 3 (1).

 Sher, R., Hoover, M.D., Newton, G.J., Rahn, F.J., 1994. Aerosol behavior in nuclear facilities. Trans. Am. Nucl. Soc. 70 (CONF-940602–).
- Sreekumar, K., Ananthapadamanabhan, P., Venkatamani, N., Joshi, P., Sapra, B., Nair, P., Nambhi, K., 1996. Plasma Torch Based Aerosol Generator. Bhabha Atomic Research Centre. BARC019960E0007.
- Suckow, D., Guentay, S., 2008. The dragon aerosol research facility to study aerosol behaviour for reactor safety applications. In: Proc. Int. Conf. Reactor Physics, Nuclear Power: A Sustainable Resource.